CHAPTER 5

Pure Nanodiamonds Produced by Laser-assisted Technique

BORIS ZOUSMAN AND OLGA LEVINSON*

Ray Techniques Ltd, The Hebrew University of Jerusalem,
P.O.B. 39162, 91391, Israel
*Email: olga.levinson@nanodiamomd.co.il

5.1 Introduction, Nanodiamond Market, Problems and Prospects

Nanodiamond powder belongs to the carbon nanomaterial family, which, along with graphene, fullerene and nanotubes, has attracted great interest in recent years due to its unique physical and chemical properties.[1–3] Initially, nanodiamond applications were rooted in the defense industry but have now reached into a variety of fields, such as fine polishing, lubricating, coatings and polymers. Currently, nanodiamonds have entered biomedicine, thermal management in electronics, photovoltaics and energy storage applications.

Nanodiamond powder is composed of diamond nanoparticles with average size of 4–5 nm, usually collected in aggregates of a few hundred nanometers and even microns. Each primary particle consists of a nanocrystal of tetrahedral bonded carbon atoms collected in a three-dimensional cubic lattice, which determines the unique properties of diamond, and an onion-like carbon shell with a chemically active ''coat'' of functional groups on the surface.[1] This coat enables interaction with various molecules, which transfers to them the unique properties of diamond and makes possible the

RSC Nanoscience & Nanotechnology No. 31
Nanodiamond
Edited by Oliver Williams

Published by the Royal Society of Chemistry, www.rsc.org

creation of novel, unique and economically viable materials and objects with desired properties.

Nanodiamond powder is one of a few nanomaterials being produced at a commercial scale. Traditionally, it is synthesized by detonation of solid explosives in metal chambers, then isolated from the obtained blend and purified in boiling acid.[1–4] Having been discovered in 1963 in the Soviet Union, nanodiamonds have been studied in depth and a lot of applications exploiting the unique nanodiamond features have been developed in the fields of fine polishing, lubrication, coatings and polymers. The potential market of nanodiamond powder is huge[4] and is estimated at 300 billion dollars annually. However, wide use of nanodiamonds is currently impeded by some problems, including:

- Low quality consistency of nanodiamonds produced by various manufacturers.
- Absence of standards for the regulation of nanodiamond quality.
- Problem of nanodiamond aggregation for most advanced applications and the absence of industrial technologies for nanodiamond dispersion within various media.
- Lack of fundamental understanding of the mechanisms influencing the structure of nanodiamonds (crystalline shape and size, thickness of sp^2 cover and type and quantity of functional groups on the surface) and the effect on the nanodiamond performance (mechanical, thermal, electrical, magnetic and optical properties of nanodiamond composites and objects).
- Insufficient quantity of already designed final nanodiamond-based products.

At the same time, recent achievements in the development of advanced nanodiamond applications[5,6] in biomedicine, photovoltaics, energy and optics present new demands on the quality of diamond nanopowder, such as the purity and homogeneity of the primary particle dimensions, as well as the surface chemistry. Due to differences in synthesis conditions, inside the detonation charge volume detonation nanodiamonds (DND) usually contain primary particles of different sizes, as well as various ratios of functional groups and sp^2 shells on the surface, which define the wide range of particle behavior in diverse reactions. An additional problem is metal impurities from the detonator and chamber materials. Insufficient levels of purity and homogeneity in DND limit the applicability and efficiency of this unique material in many important fields, such as heat conductive insulating compounds and fine polishing materials for electronics, nuclear fuel, electrodes for efficient energy storage, cold emitters for displays, photovoltaic elements, terahertz radiation sensors, agents for high performance liquid chromatography, diagnostic kits and drugs. Moreover, detonation technology is dangerous, polluting and requires additional expenses for safety and security. Apart from the non-controllable character of the detonation

process, insufficient quality, safety and regulatory issues, the cost of DND is relatively expensive for some applications.

Special techniques for DND unification and fractionalization should be developed, as well as special standards ensuring ND quality. These activities may subsequently raise the price of already expensive DND. Therefore, novel technologies for nanodiamond fabrication, enabling control of the synthetic process, to increase the quality of the product and to reduce its cost are currently of particular importance.

5.2 Synthesis Nanodiamonds by Laser Ablation in Liquid

Laser ablation has been studied from the creation of ruby lasers in the sixties of the last century and is currently widely used for analytical spectroscopy,[6] surface treatment, coatings and the synthesis of nanomaterials.[7] The synthesis of nanoparticles by laser ablation in liquid (PLAL), named also liquid-phase pulse laser ablation (LP-PLA) and the pulsed-laser-induced liquid–solid interfacial reaction (PLIIR), was first reported in 1987 when a metastable form of iron oxide was obtained by high-power pulsed-laser radiation of liquid–solid interfaces.[8] Since then, interest in this method of synthesis has been steadily increasing.[9,10] The synthesis of nanoscale particles of silver,[11] gold,[12] cubic-boron nitride,[13] titanium dioxide,[14] cobalt oxide,[15] cubic-carbon nitride[16] and other nanostructures[8] has been reported in various publications. Special interest regarding this method for nanoparticle fabrication was ignited by the possibility to control the parameters of the obtained nanostructures, such as their size, morphology and shape, by adjusting the parameters of laser radiation, the liquid and the target. This control is highly important for most nanomaterial applications, such as nano-biosurgery and light emission.

In this method a pulsed laser beam of high density is focused onto the surface of a solid target, which is placed in a liquid. The interaction of the laser beam and the target surface can result in vaporization of the target in the form of an ablation plume. Atoms of the target and liquid interact under high pressure and high temperature conditions, allowing the formation of nanoparticles dispersed in suspension.

The PLAL technique for producing nanodiamonds has been studied by several academic groups.[15–18] Theoretical and experimental justifications for the growth of diamond nanocrystals *via* PLAL have been performed in order to predict the size of primary particles and the yield of the process.[7,9,10,26,27] It was shown that the growth of diamond crystals is followed by the formation of single nanocrystals and twin structures, including a single twin and triple twin, as well as four- and five-fold twin structures.[25,26] Nanodiamond particles of various sizes were obtained using laser Nd-YAG radiation with different parameters and in diverse liquids (Table 5.1). However, to the best of our knowledge, attempts to synthesize nanodiamonds by this method proved to be economically impractical.

Table 5.1 Nanodiamond synthesis by PLAL reported earlier.

#	*Wavelength, nm*	*Repetition frequency, Hz*	*Power density, W cm^{-2}*	*Pulse width*	*Graphite target*	*Liquid*	*ND size, nm*	*Author, year*	*Ref.*
1	532	5	10^{11}	10 nc	Poly-crystalline	Water	300–400	G. W. Yang, 1998, 2000	19, 20
2	532	5	10^{11}	10 nc	Poly-crystalline	Acetone	30–40	G. W. Yang, 2002	21
3	532	10	66 J cm^{-2} Spot: 0.5 mm 6.6×10^{9}	10 nc	Graphite disk	Water	?	P. W. May, 2004	22
4	532	10	66 J cm^{-2} Spot: 0.5 mm 6.6×10^{9}	10 nc	Graphite disk	Cyclo-hexane (in Ar)	?	P. W. May, 2004	22
5	532	?	28 J cm^{-2} Spot: 0.5 mm	15 nc	Graphite	Water	~100	P. W. May, 2006	15
6	1064	20	4×10^{6} W cm^{-2}	1.2 ms	Graphite particles <2.0 μm	Water	3–6	Xi-Wen Du, 2006	23
7	355	10	40–1000 J cm^{-2} Spot: 0.1–0.5 mm	5 nc	Pyrolytic graphite	Water?	5–15	Olivier Guillois, 2008	18
8	1064	20	4×10^{6} W cm^{-2}	0.4 ms	Graphite particles <2.0 μm	Water	2–7	P. Bai, 2010	25
9	1064	20	4×10^{6} W cm^{-2}	1.2 ms	Graphite particles <2.0 μm	Water	2–13	P. Bai, 2010	25

5.3 Light Hydro-dynamic Pulse for Nanodiamond Fabrication

In this work we describe a novel approach to produce nanodiamonds by a controlled synthesis. The proposed method is a form of PLAL; however, at the same time, two main innovations change the physics of the process, which allow us to describe this as a new method of synthesis, named light hydro-dynamic pulse (LHDP). The new approach is based on the treatment of a specially prepared multi-component solid target, containing a carbon non-diamond source, by a radiation beam focused in a transparent liquid at some predetermined distance from the target surface. In this case the formation of diamond nanocrystals is not the result of the plasma treatment of graphite as happens in reported experiments with PLAL, but as a consequence of the impact of an acoustic shock wave created by plasma on the surface of the composite material containing carbon black and hydrocarbons.

The treatment of specially prepared multi-component targets, rather than graphite, as was done earlier, by acoustic shock waves and not by plasma has led to a considerable increase in productivity, which offers the prospect of industrial implementation of the laser nanodiamond synthesis.

5.3.1 Technological Process

Presently, nanodiamonds are produced by LHDP synthesis under laboratory conditions. The process consists of the following operations:

1. Formation of a special target from pure carbon soot and a hydrocarbon binder.
2. Laser treatment of targets in liquid accompanied by ND synthesis and the production of a carbon blend that is free of metals.
3. Removal of hydrocarbons; isolation of synthesized nanodiamonds from the blend.
4. Washing and drying.

The targets are prepared with commercially available soot and wax in a 50/50 weight content by heating and mixing. Various additives (stearic acid, fullerenes, urea, naphthalene, *etc.*) can be used to increase the productivity or provide specific surface chemistry. Then, the mixture is poured into a glass bowl and, after drying, the bowl with the prepared target is filled with glycerin or water.

The treatment of the targets is conducted by a series of laser pulses of specific parameters in liquid media at room temperature and under normal pressure. We use a YAG solid-state laser with a wavelength of 1064 nm and laser pulse intensity of 1010 W cm^{-2}. The target is fixed on the table, which moves automatically so that the laser spot scans in the fluid at a distance of 3 mm above the target surface.

After removal of the hydrocarbons with an organic solvent, the synthesized NDs are isolated from the non-diamond carbon particles by flotation. Then, the NDs are rinsed with deionized water and dried.

5.3.2 Physical Mechanism

The specially prepared target is placed in a liquid media and a laser beam of specific parameters is focused at the some predetermined distance from the target surface. The laser beam leads to the emergence of acoustic shock waves of high power that impact on the target surface and provide specific conditions (*e.g.*, temperature, pressure, *etc.*) that are sufficient for the formation of the diamond cubic crystal structure of carbon. This happens when the specific ratio of the liquid refractive index and the light flow intensity provides a self-focusing effect and a laser beam energy of high density is absorbed at the focus. This energy concentrated at the focus area causes a rapid jump of the temperature and liquid evaporation, which results in a shock wave of high power (light hydraulic effect) and sound excitation.[30] This is the acoustic shock wave in front of which carbon atoms of the target are collected in a cubic diamond structure, forming nanocrystals. This happens due to the thermo-mechanical instability characterized by the highly inhomogeneous space distribution of both the pressure (P) and temperature (T) of the target mixture. As the duration of the laser pulses is rather short, the time derivatives of both the pressure (dP/dt) and the temperature (dT/dt) are extremely high and both P and T rise dramatically in certain micro-regions, reaching values in which the thermodynamically stable form of carbon is a diamond.

Contrary to the existing technology for nanodiamond fabrication by detonation, LHDP is environmentally friendly and not dangerous. No explosives are needed and the crystalline sizes can be controlled. Depending on the parameters of laser radiation, nanodiamonds with an average size of 4–5 nm size or 250–300 nm can be obtained by this method. The crystal sizes have been confirmed by transmission electron microscopy (Figure 5.7).

5.4 Characterization of Nanodiamonds Obtained by Laser Synthesis

5.4.1 X-Ray Diffraction (XRD) Analysis

The crystalline structure of laser nanodiamonds (LND) was determined by X-ray diffractometry (D8 Advance, Bruker AXS) in Cu Kα radiation (Figure 5.1). The XRD pattern obtained for the samples indicates that the powder consists of only a crystalline phase, *i.e.*, the diamond crystal lattice (identified with JCPDS card 6–675).

A lattice constant of 0.35687 Å was calculated with a Rietveld refinement using TOPAS software, which also indicated a cubic diamond structure.

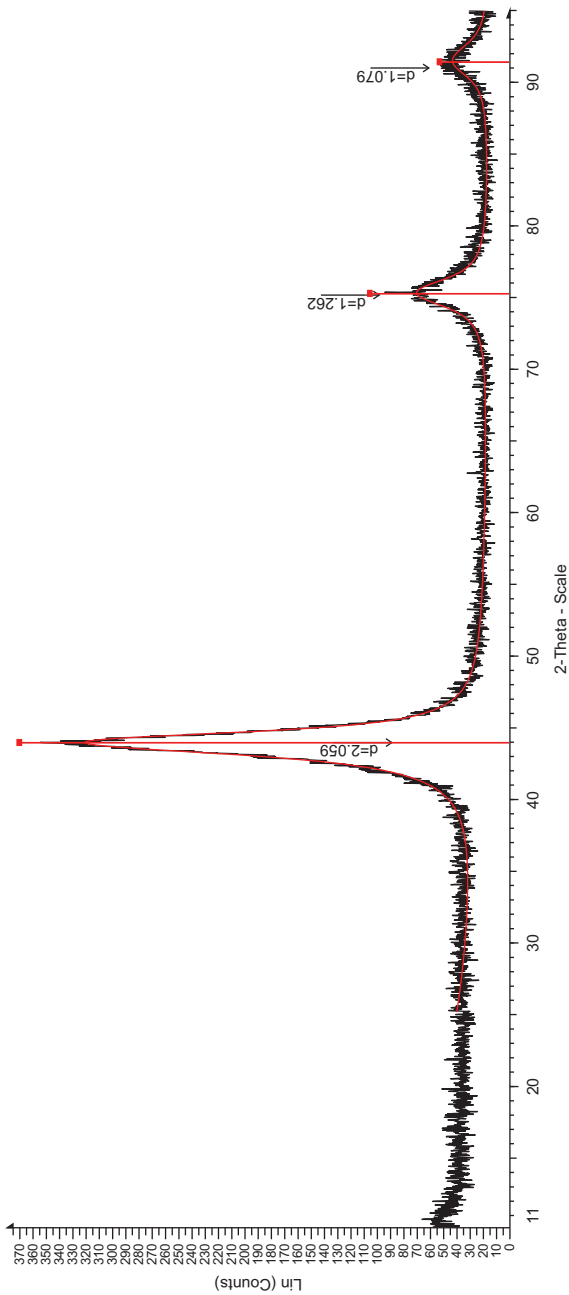

Figure 5.1 XRD analysis.

The absence of non-diamond peaks and troughs is evidence of the high purity and fine crystallinity of the LND powder. The average diamond crystallite size was evaluated from the full width half maxima (FWHM) of the peaks, which appeared on the diffraction pattern at angles of 44.01 and 75.34° (2Theta scale) and grain size values of 4.3 and 3.7 nm, respectively, were calculated.

5.4.2 Scanning Electron Microscopy

Scanning electron microscopy (SEM) was performed using a high-resolution microscope (SEM Serion) with energy dispersive X-ray spectroscopy (EDS) and Magellan™ 400L (Figure 5.2). The Serion image (Figure 5.2a) shows that the powder consists of agglomerates with a size of more 1 μm. Microanalysis EDS (Figure 5.2b) indicated the high purity of the local area and did not identify any other elements, except for carbon, oxygen and nitrogen. To see the samples in high resolution, dry nanodiamond powder was placed on a special grid (Figure 5.2c) and observed with the Magellan. The three-dimensional images show aggregates with a size of 25–400 nm (Figure 5.2d).

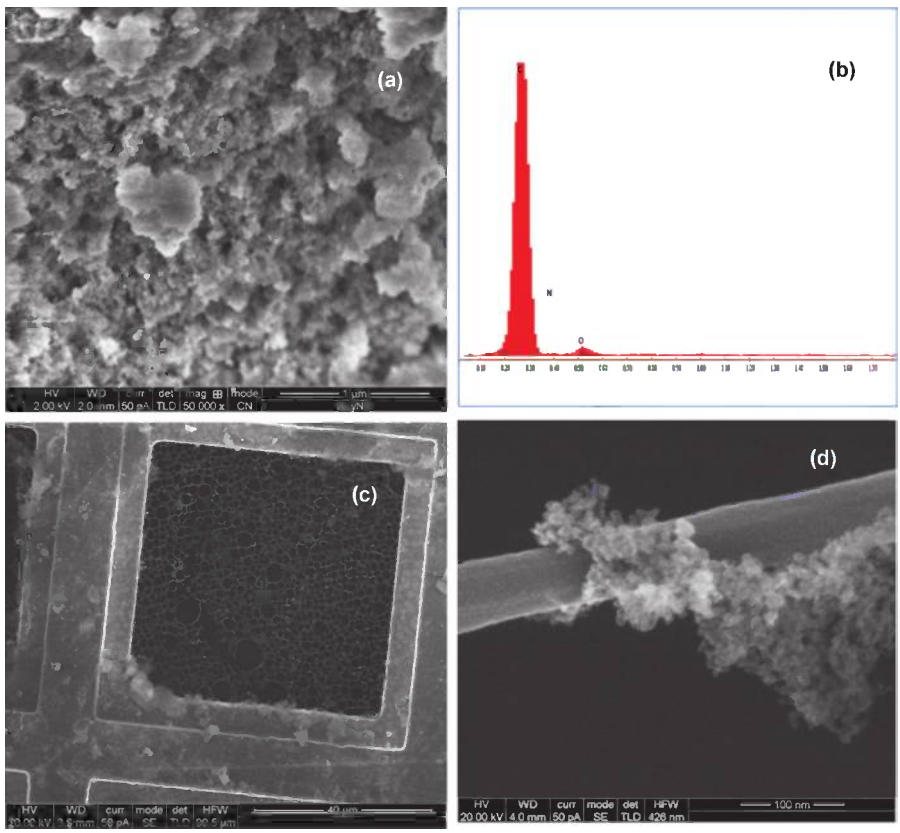

Figure 5.2 Scanning electron microscopy.

The aggregates consist of nanoparticles with an average size of around 4–5 nm. They are usually collected in small, highly porous aggregates, which in turn form big agglomerates, as shown in the Serion image.

5.4.3 Transmission Electron Microscopy

The dry nanodiamond powder was investigated by high resolution transmission electron microscopy (HRTEM; Tecnai F20 G2). The obtained TEM images (Figure 5.3 and Figure 5.4) are similar to DND.[28] They show that the material consists of porous agglomerates in which primary particles with a nanoscale size from 2–3 to 15–17 nm have a clearly observable crystalline lattice and contact with one another through some kind of disordered material, with no evidence of periodicity. Crystalline regions are noted to sometimes consist of twinned structures with a size of 10–20 nm. The size distribution of the crystallites with visible lattice fringes was determined by TEM point counting. The maximum of the distribution was at around 4–5 nm, which coincides with the results obtained from the XRD data.

Electron energy-loss spectroscopy (EELS) was used to determine the bonding of LND. It was found (Figure 5.5) that the EELS spectrum looks very similar to the results of the DND analysis: a pre-peak in the region of 285–290 eV, a core-loss peak at 300 eV, which characterizes ND at the core-loss range, a main peak in the region of 300 eV and ''sole'' and twin peaks in the regions of 315 and 335 eV, respectively. The small peak in the region of 410 eV[1] shows some slight presence of nitrogen vacancy (NV) defects in the nanodiamond grains.[31] The small dimensions of the pre-peak at 285–290 eV are indicative of the very low content of non-diamond structures on the surface compared with DND.[1]

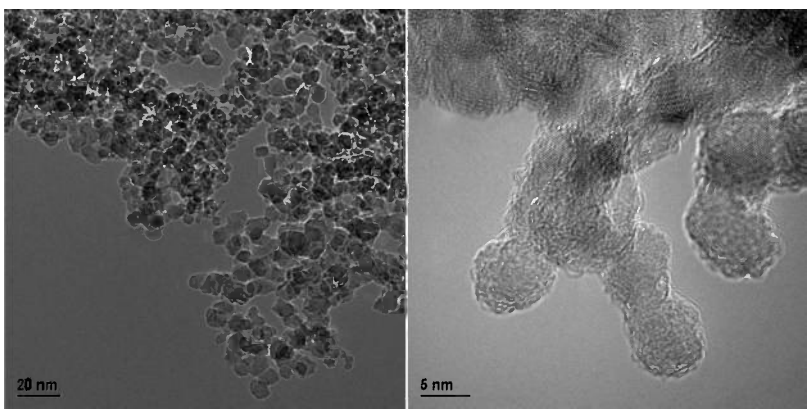

Figure 5.3 TEM images with 20 nm and 5 nm scale bars.

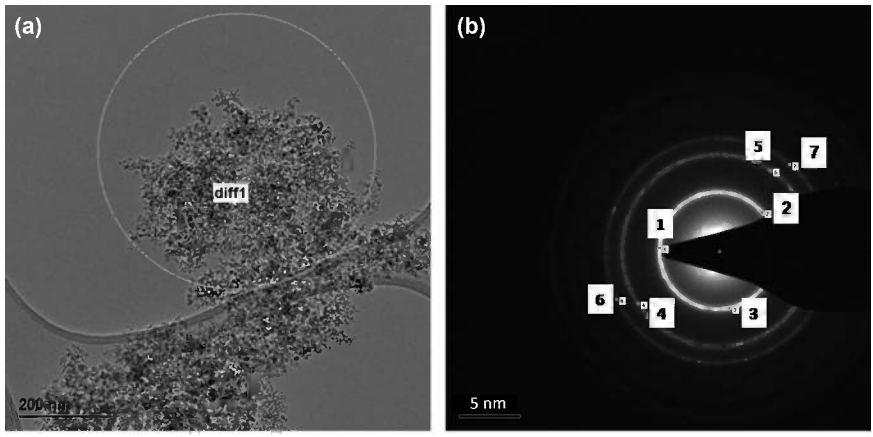

(c)	Measured spacing, nm	Miller index
1	0.2026	111
2	0.2101	111
3	0.2108	111
4	0.1261	220
5	0.1274	220
6	0.1072	311
7	0.1089	311

Figure 5.4 Selected area electron diffraction (SAED): a) selected area, b) electron diffraction pattern, c) measured interplanar spacings.

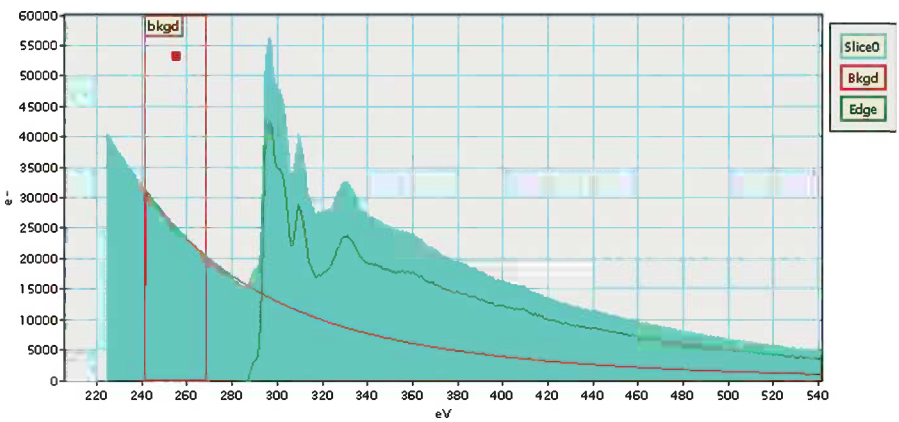

Figure 5.5 EELS.

5.4.4 Raman Spectroscopy

Raman spectroscopy analysis was performed using a Raman microscope (WITec GmbH) with an excitation wavelength of 488 nm and a power of 1 mW (Figure 5.6). In contrast to the Raman shift of purified DND,[5] the diamond peak at 1323 cm^{-1} is much higher than that of the sp^2 peak at 1590 cm^{-1}. This indicates a higher content of the diamond phase compared to DND.

5.4.5 Inductively Coupled Plasma Mass Spectrometry

Metal impurities were determined by inductively coupled plasma mass spectrometry (ICP-MS; Agilent 7500cx). The averages of three measurements are presented in the Table 5.2.

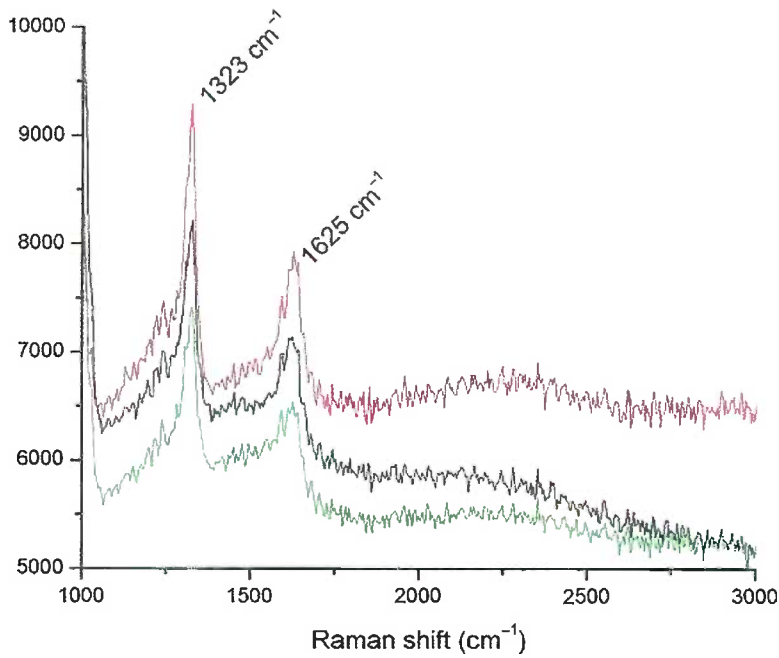

Figure 5.6 Raman spectra.

Table 5.2 ICP analysis to show the metal impurities.

Element	*Zn*	*Ni*	*Mn*	*Fe*	*Cr*	*Al*
Blank, ppm	<1	<2	<1	<1	<2	<5
LND, ppm	44	20	35	45	114	19

5.5 Controlled Nanodiamond Synthesis

The LHDP process of LND synthesis can be controlled by varying at least one of the following parameters:

- Content of the specially prepared carbon source target.
- Optical and mechanical characteristics of the liquid media.
- Width and/or shape of the laser pulse.
- Energy flux.
- The distance between the focusing plane and the surface of the solid carbon-source target.

Changing these parameters affects the size of the obtained diamond nanocrystals, the size of the shell and the character of functional groups on the crystal surface. These features define the interactions that nanodiamonds have with each other (aggregation) and with other particles, as well as their performance in applications.

As has been reported in previous investigations using PLAL,[24] the pulse width affects the size of the synthesized nanodiamonds. LNDs of different sizes (Figure 5.7) were obtained by LHDP when the target, liquid, focus location and light were kept constant. Just enhancing the pulse width resulted in a significant increase in the size of the nanodiamonds and in their magnetic resonance (Figure 5.8), which was studied earlier.[28,29] These special LNDs were analyzed by electron paramagnetic resonance (EPR) spectroscopy and compared with DND. The EPR spectra are shown in Figure 5.8. LNDs demonstrate enhanced paramagnetism compared with DND. The special LND spectrum, in contrast to normal LND and DND, shows a hyperfine pattern, usually attributed to NV paramagnetic centers.[29,30]

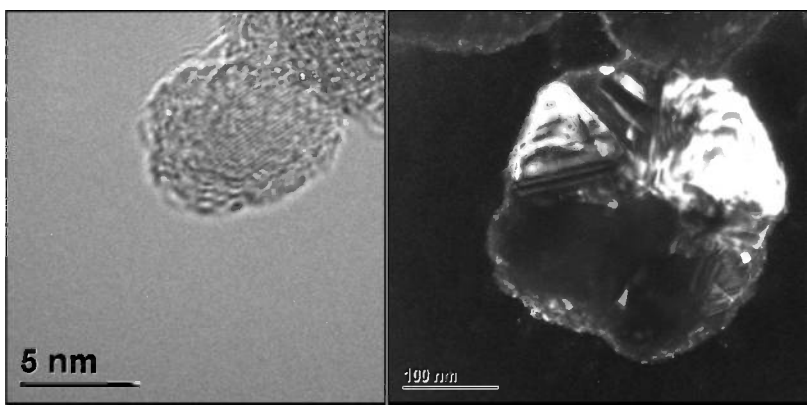

Figure 5.7 HRTEM images of LND on the left and LND obtained under an enhanced pulse width on the right.

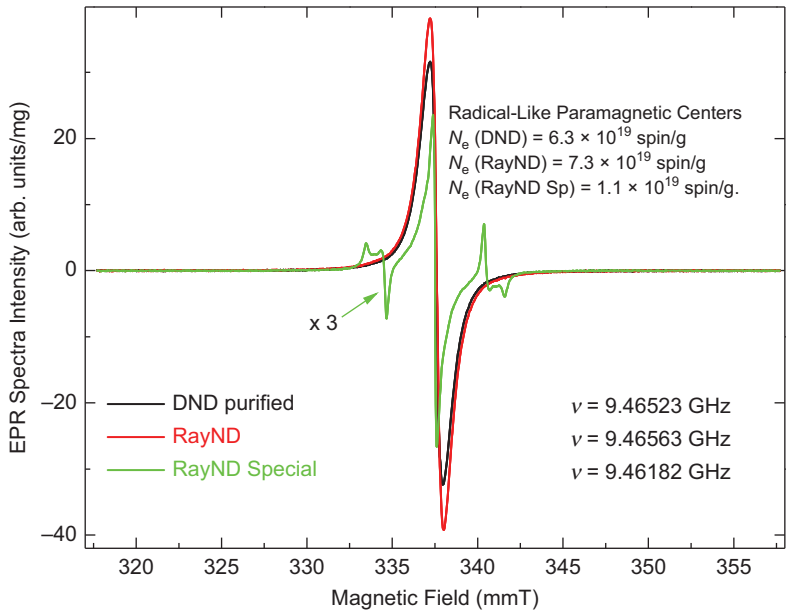

Figure 5.8 EPR spectra of LND (RayND) and DND samples.

5.6 LHDP *vs.* Existing Technology for Detonation Nanodiamond Synthesis

Table 5.3 summarizes the main advantages of LHPS over the detonation synthesis approach.

Table 5.3 Comparison of detonation synthesis and light hydrodynamic pulse synthesis.

Detonation Synthesis: mass production	*Light Hydrodynamic Pulse Synthesis: laboratory fabrication*
1. Raw material: explosives (trinitrotoluene, TNT; cyclotrimethylenetrinitramine, RDX); hazardous and polluting technology	1. Raw material: carbon soot and hydrocarbon binder; environmentally friendly technology
2. Uncontrolled synthesis a) Size distribution non-constant b) High variability of surface chemistry	2. Controlled synthesis a) Size distribution can be controlled (Figure 5.7) b) Controlled surface chemistry
3. Insufficient (non-constant) quality: a) Incombustible residue: 0.2–1.4 wt.% b) Metal impurities c) Low homogeneity d) Presence of polycrystals	3. High quality: a) Incombustible residue: <0.01 wt.% b) Near metal free c) High homogeneity d) Polycrystal free
4. Limited scope of possible applications	4. Wide scope of possible applications
5. Difficulties for implementation	5. Ease for implementation
6. Problematic to reduce cost; additional security expenses	6. Highly competitive when produced on an industrial scale

5.7 Conclusion and Prospects in the Development of the Nanodiamond Industry

A novel laser synthesis technology for nanodiamond powder fabrication has been developed. The technology is environmentally friendly and non-hazardous, enables control over the diamond nanocrystal dimensions and defects, and allows nanodiamonds of high purity to be obtained, which are metal- and graphite-free with high homogeneity.

The possibility to control the characteristics of nanodiamond are very important for most advanced applications, such as:

- Optics: better surface control important for IR and visible spectra.
- Thermal management in heat capacitors and heat conductors: LND is more pure and has a narrower size distribution and, as a result, holds more promise for high thermo-conductivity.
- Biomedical and biochemical fields: better promise due to the purity and enhanced size control.
- Mechanical (production of polymers, lubricants, polish components and additives for coatings): LND better due to the higher homogeneity and dispersion.

After transition to a mass production, the cost of LND powder is expected to drop considerably. The low price, together with the possibility of controlling the dimensions and surface chemistry, will ensure the rapid development of advanced ND applications, such as drug and gene delivery agents, biosensors and diagnostic kits, optical filters and photovoltaic elements, thermal interface materials and heat sinks for electronics, field emission displays, and quantum computers.

Acknowledgments

We thank to Dr Elena Perevedentseva for the analysis of LND samples and who kindly provided the Raman spectroscopy results. We also thank to Dr Alexander Shames for the comparative EPR analysis of LND and DND samples.

References

1. O. Shenderova and D. Gruen, *Ultrananocrystalline Diamond: Synthesis, Properties and Applications*, William Andrew, 2006.
2. A. M. Schrand, S. A. Ciftan Hens and O. A. Shenderova, *Critical Rev. Solid State Mater. Sci.*, 2009, **34**, 18.
3. M. Baidakova and A. Vul, New prospects and frontiers of nanodiamond clusters, *J. Phys. D: Appl. Phys.*, 2007, **40**, 6300–6311.
4. V. V. Danilenko, Detonation nanodiamonds: problems and prospects, *Superhard Materials*, 2010, **N5**.

5. V. N. Mochalin, O. Shenderova, D. Ho and Y. Gogotsi, The properties and applications of nanodiamonds, *Nat Nanotechnol.*, 2012, **7**(1), 11–23.
6. B. C. Windom and D. W. Hahn, Laser ablation—laser induced breakdown spectroscopy (LA-LIBS): A means for overcoming matrix effects leading to improved analyte response, *J. Anal. At. Spectrom*, 2009, **24**, 1665–1675.
7. G. W. Yang, Laser ablation in liquids: Applications in the synthesis of nanocrystals, *Prog. Mater. Sci.*, 2007, **52**(5), 648–698.
8. P. P. Patil, D. M. Phase, S. A. Kulkarni, S. V. Ghaisas, S. K. Kulkarni, S. M. Kanetkar, S. B. Ogale and V. G. Bhide, Pulsed-laser-induced reactive quenching at liquid-solid interface: aqueous oxidation of iron, *Phys. Rev. Lett.*, 1987, **58**, 238.
9. H. Zeng, X.-W. Du, S. C. Singh, S. A. Kulinich, S. Yang, J. He and W. Cai, Nanomaterials via Laser Ablation/Irradiation in Liquid: A Review, *Adv. Funct. Mater.*, 2012, **22**, 1333–1353.
10. G. Yang (ed.), *Laser Ablation in Liquids, Principles and Applications in the Preparation of Nanomaterials*, Pan Stanford Publishing, Singapore, 2012.
11. A. Pyatenko, K. Shimokawa, M. Yamaguchi, O. Nishimura and M. Suzuki, Synthesis of silver nanoparticles by laser ablation in pure water, *Appl. Phys. A.*, 2004, **79**, 803.
12. T. E. Itina, On Nanoparticle Formation by Laser Ablation in Liquids, *J. Phys. Chem. C*, 2011, **115**, 5044.
13. J. B. Wang, G. W. Yang, C. Y. Zhang, X. L. Zhong and Z. H. A. Ren, Symmetric organization of self-assembled carbon nitride, *Chem. Phys. Lett.*, 2003, **367**, 10.
14. C. H. Liang, Y. Shimizu, T. Sasaki and N. Koshizaki, Preparation of ultrafine TiO2 nanocrystals via pulsed-laser ablation of titanium metal in surfactant solution, *Appl. Phys. A*, 2005, **80**, 819.
15. L. Yang, P. W. May, L. Yin, J. A. Smith and K. N. Rosser, Growth of diamond nanocrystals by pulsed laser ablation of graphite in liquid, *Diamond & Related Materials*, 2007, **16**, 725–729.
16. J. Sun, S.-L. Hu, X.-W. Du, Y.-W. Lei and L. Jiang, Ultrafine diamond synthesized by long-pulse-width laser, *Appl. Phys. Lett.*, 2006, **89**, 183115.
17. S. Hu, J. Sun, X. Du, F. Tian and Lei, The formation of multiply twinning structure and photoluminescence of well-dispersed nanodiamonds produced by pulsed-laser irradiation, *Diamond & Related Materials*, 2008, **17**, 142.
18. D. Amans, A. Chenus, G. Ledoux, C. Dujardin, C. Reynaud, O. Sublemontier, K. Masenelli-Varlot and O. Guillois, Nanodiamond synthesis by pulsed laser ablation in liquids, *Diamond & Related Materials*, 2009, **18**, 177–180.
19. G.-W. Yangyz, J.-B. Wangy and Q.-X. Liuy, Preparation of nano-crystalline diamonds using pulsed laser induced reactive quenching, *J. Phys.: Condens. Matter.*, 1998, **10**, 7923–7927.

20. G. W. Yang and J. B. Wang, Pulsed-laser-induced transformation path of graphite to diamond via an intermediate rhombohedral graphite, *Appl. Phys. A*, 2001, **72**, 475.
21. J. B. Wang, C. Y. Zhang, X. L. Zhong and G. W. Yang, Cubic and hexagonal structures of diamond nanocrystals formed upon pulsed laser induced liquid–solid interfacial reaction, *Chemical Physics Letters*, 2002, **361**, 86.
22. S. R. J. Pearce, S. J. Henley, F. Claeyssens, P. W. May, K. R. Hallam, J. A. Smith and K. N. Rosser, Production of nanocrystalline diamond by laser ablation at the solid liquid interface, *Diamond and Related Materials*, 2004, **13**, 661.
23. J. Sun, S.-L. Hu, X.-W. Du, Y.-W. Lei and L. Jiang, Ultrafine diamond synthesized by long-pulse-width laser, *Appl. Phys. Lett.*, 2006, **87**, 183115.
24. P. Bai, S. Hua, T. Zhang, J. Sun and S. Cao, Effect of laser pulse parameters on the size and fluorescence of nanodiamonds formed upon pulsed-laser irradiation, *Materials Research Bulletin*, 2010, **45**, 826.
25. C. X. Wang, Y. H. Yang and G. W. Yang, Thermodynamical predictions of nanodiamonds synthesized by pulsed-laser ablation in liquid, *J. Appl. Phys.*, 97, 2005, **6**, 066104.
26. C. X. Wang, P. Liu, H. Cui and G. W. Yang, Nucleation and growth kinetics of nanocrystals formed upon pulsed-laser ablation in liquid, *Appl. Phys. Lett.*, 2005, **87**, 201913.
27. Q. Zou, Y. G. Li, L. H. Zou and M. Z. Wang, Characterization of structures and surface states of the nanodiamond synthesized by detonation, *Materials Characterization*, 2009, **60**(11), 1257–1262.
28. L. B. Casabianca, A. I. Shames, Alexander M. Panich, O. Shenderova and L. Frydman, Factors affecting DNP NMR in Polycrystalline Diamond Samples, *J. Phys. Chem. C*, 2011, **115**(39), 19041–19048.
29. A. Panich, A. Shames, B. Zousman and O. Levinson, Magnetic resonance study of nanodiamonds prepared by laser-assisted technique, *Diamond and Related Materials*, 2012, **23**, 150–153.
30. ''Science Discovery'' under number No. 65 in the name of; G. A. Askar'yan, A. M. Prokhorov, G. F. Chanturiya and G. P. Shipulo, The effects of a laser beam in a liquid, *Sov. Phys. JETP*, 1963, **17**(6), 1463–1465.
31. I. I. Vlasov, O. Shenderova, S. Turner, O. I. Lebedev, A. A. Basov, I. Sildos, M. Rähn, A. A. Shiryaev and G. Van Tendeloo, *Small*, 2010, **6**(5), 687.